## Title
Effects of Induced Astigmatism on Spectral Domain-OCT Angiography Quantitative Metrics



## Authors
Jung, Jesse J
Soh, Yu Qiang
Sha, Patricia
et al.

## Publication Date
2020-11-01

## DOI
10.1016/j.ajo.2020.07.005

Peer reviewed

HHS Public Access

Author manuscript

*Am J Ophthalmol*. Author manuscript; available in PMC 2021 November 01.

Published in final edited form as:

*Am J Ophthalmol*. 2020 November ; 219: 49–58. doi:10.1016/j.ajo.2020.07.005.

# Effects of Induced Astigmatism on Spectral Domain-OCT Angiography Quantitative Metrics

**Jesse J. Jung**[1,2], **Yu Qiang Soh**[3], **Patricia Sha**[4,5], **Sophia Yu**[4], **Mary K. Durbin**[4], **Quan V. Hoang**[3,6]

[1]East Bay Retina Consultants, Inc., Oakland, CA, USA

[2]Department of Ophthalmology, Universtiy of California, San Francisco, San Francisco, CA, USA

[3]Singapore Eye Research Institute, Singapore National Eye Centre, Duke-NUS Medical School, Singapore

[4]Carl Zeiss Meditec, Inc.

[5]Silicon Valley Eyecare Optometry, CA, USA

[6]Department of Ophthalmology, Edward S. Harkness Eye Institute, Columbia College of Physicians and Surgeons, NY, USA

## Abstract

**Purpose:** To analyze the effect of induced astigmatism on en-face spectral-domain optical coherence tomography angiography (SD-OCTA) quantitative metrics.

**Design:** Prospective Cross-Over Study

**Methods:** Normal eyes without astigmatism and with 0.75, 1.75, and 2.75 diopters (D) of with-the-rule (WTR) astigmatism were imaged utilizing a 3×3mm scan pattern SD-OCTA CIRRUS™ 5000 HD-OCT with AngioPlex (Carl Zeiss Meditec, Dublin, CA, USA). Quantitative parameters including foveal avascular zone (FAZ) metrics, parafoveal vessel length density (VD), and perfusion density (PD) were corrected for magnification secondary to axial length and analyzed. Univariate linear regressions were performed within each eye to correlate quantitative metrics to level of induced astigmatic cylinder.

**Results:** 15 eyes (15 patients) were imaged. Every 1D increase in induced WTR astigmatism was associated with a statistically significant decrease in VD and PD within all ETDRS (Early Treatment Diabetic Retinopathy Study) inner-ring quadrants, however especially so nasally (VD: 0.63, $p<0.001$; PD: 0.0089, $p = 0.001$). For every 1D increase in induced astigmatism, the resulting decrease in the inner-ring superior quadrant was 12% greater for VD and 16% greater for PD

Correspondence/reprints should be addressed to: Jesse J. Jung, M.D., East Bay Retina Consultants, Inc., 3300 Telegraph Ave., Oakland, CA 94609, Phone: 510-444-1600, Fax: 510-444-5117, jung.jesse@gmail.com.

versus the inferior quadrant; the resulting decrease in the inner-ring nasal quadrant was 40% greater for VD and 48% greater for PD versus the temporal quadrant.

**Conclusions:** Increasing levels of induced WTR astigmatism correlate with globally diminishing VD and PD, more symmetrically for vertical than horizontal quadrants, and most pronounced nasally. This may be due to a high prevalence of horizontally-oriented vessels nasally, and the horizontal optical defocus induced by WTR astigmatism.

### Keywords

Astigmatism; Against-the-Rule; Spectral-Domain Optical Coherence Tomography Angiography; Vessel Density; Perfusion Density; With-the-Rule

## Introduction

Optical coherence tomography angiography (OCTA) allows for non-invasive evaluation of the retinal vascular architecture and flow patterns based on signal decorrelation characteristics across a set of successively acquired, high-resolution cross-sectional retinal images.[1] Major advantages of OCTA over traditional fundus fluorescein angiography include rapid image acquisition,[2] depth-resolved image segmentation[1] – in particular the ability to clearly image the deep capillary networks,[3] as well as the avoidance of discomfort due to intravenous exogenous fluorescein dye injection and associated risk of rare life-threatening allergic reactions.[4,5] Over the past decade, OCTA has been utilized for the diagnosis and monitoring of a wide range of retinal pathologies such as retinal artery[6] or vein occlusions,[7–11] choroidal neovascularization,[12–14] retinal angiomatous proliferations,[15,16] polypoidal choroidal vasculopathy[1,17,18], inflammatory conditions such as idiopathic multifocal choroiditis,[19,20] and diabetic retinopathy.[21–25]

However, OCTA is also known to be associated with a spectrum of image acquisition and processing artifacts which may negatively affect its reproducibility and reliability.[1,26,27] For example, image distortion arising from patient movement during OCTA acquisiton may result in a lower-than-expected vascular density.[26] Low signal strength can affect the quality and reliability of quantitative metrics.[28] Defocus,[29] uncorrected axial length,[30] or media opacities in the vitreous and crystalline lens may result in the false appearance of a global vascular dropout.[31,32] Decentration, refraction shift and tilt are also known to contribute towards poor image quality and result in non-reproducible readings across sequential imaging sessions.[33] Nonetheless, most of these artifacts including decentration, refraction shift, tilt, and even those classified as severe artifacts such as shadow and defocus, can be corrected or mitigated by proper technician training and patient coaching.[26]

Refractive status such as axial myopia has been shown to be associated with changes in OCTA metrics such as reduced vessel density and enlarged foveal avascular zone (FAZ), possibly due to underlying anatomical alterations in keeping with pathological myopia which may over time, progress to myopic maculopathy.[30,34–39] Additionally, uncorrected spherical refractive defocus also affects OCTA image quality and can lead to an erroneous underestimation of vessel and perfusion density.[29] However, the exact correlation between the severity of astigmatic defocus and its effect on OCTA quantitative metrics has not been

elucidated. In contrast to spherical defocus which results in a uniform optic blur, cylindrical defocus induces a varying gradient of optical blur across different meridians within the 3×3 mm OCTA scan area. Accordingly, we hypothesized that the presence of cylindrical defocus results in an apparent decrease in vessel density on OCTA, albeit to a varying degree across the vertical and horizontal quadrants.

## Methods

This prospective, cross-over, single-center clinical practice cohort study received prospective institutional review board (IRB) approval from Salus IRB (Austin, TX). This study complied with the Health Insurance Portability and Accountability Act of 1996 and followed the tenets of the Declaration of Helsinki. All individuals signed a written informed consent prior to participating in the study.

### Participants

Healthy eyes without significant astigmatism or intraocular pathologies were eligible for this study. Each eligible eye underwent non-mydriatic, auto-refraction (Visuref 100, Carl Zeiss Meditec, CA, USA) to measure the amount of spherical and astigmatic correction. In addition, optical biometry including axial length measurements were obtained with IOL Master 700 (Carl Zeiss Meditec, Dublin, CA, USA). While there were no restrictions on spherical refractive errors, eyes were excluded if total astigmatism exceeded 0.25 diopters (D).

### Optical Coherence Tomography Angiography Imaging

Each eye underwent spectral-domain OCTA (SD-OCTA) with the CIRRUS™ 5000 Angioplex (Carl Zeiss Meditec, Dublin, CA, USA). SD-OCTA scanning was performed over a 3×3 mm region centered at the FAZ. All eyes were centered on the fovea and SD-OCTA scans with high quality were obtained. Images were accepted only if they exhibited signal strength of 8 or higher (maximum signal strength for the AngioPlex software is a value of 10), had correct segmentation, uniform illumination without areas of darkness, foveal centration, and minimal artifacts or saccades (identified as horizontal misalignment of vessel segments on en-face images). All images were obtained using the default commercial automated segmentation boundaries, and standard tracking software was utilized to minimize motion artifacts. Each en-face SD-OCTA image was generated using the optical microangiography (OMAG©, Carl Zeiss Meditec, Dublin, CA, USA) algorithm at a resolution of 1024 × 1024 pixels, using 245 A-scans acquired at 245 B-scan positions. Each eye underwent SD-OCTA imaging at its baseline refractive error without astigmatism, followed by repeated imaging in the presence of with-the-rule (WTR) astigmatism induced via toric contact lenses of increasing power (0.75, 1.75 and 2.75 D) in a randomized order to ensure the effect was not due to increased chair time or fatigue.

### Quantitative Measurements

Regional analysis was performed following segmentation of the superficial retinal layer (SRL) in each SD-OCTA image, based on the Early Treatment of Diabetic Retinopathy Study (ETDRS) parafoveal inner ring and central subfield. The ETDRS central subfield was

defined as a central circle measuring 1000 μm in diameter, centered at the fovea. The ETDRS inner ring was defined as a concentric ring with an inner diameter of 1000 μm and an outer diameter of 3000 μm centered at the fovea. The inner ring was further divided as 4 equal quadrants (superior, inferior, nasal, temporal) for sub-region analysis. ETDRS full ring was defined as the combined area represented by both the inner ring and central subfield. Each en-face SD-OCTA image was digitally analyzed with the Zeiss AngioPlex algorithm (version 10.0; available via a research license but not available in all markets, Carl Zeiss Meditec, Dublin, CA, USA) to quantify FAZ characteristics, SRL vessel length density (VD), and SRL perfusion density (PD). FAZ characteristics included size, perimeter, and circularity. Circularity was defined as the measure of the shape of the FAZ relative to a circle, with a higher value corresponding to a more circular shape. VD was defined as the total length of perfused vasculature per unit area of the image ($mm^{-1}$). PD was defined as the total area covered by perfused vasculature per unit area (unitless).

Quantitative metrics were corrected for the magnification factor due to variation in axial length as described by Sampson and colleagues[30] using the Littman and modified Bennett formulae for the Zeiss AngioPlex (default axial length 24.46 mm, Carl Zeiss Meditec, Dublin, CA, USA): $D_t^2/D_m^2 = 0.001949*(AL-1.82)^2$; where $D_t$ is the true physical linear dimension of the fundus, $D_m$ is the measured OCTA image diameter, 1.82 is a constant related to the distance between the corneal apex and the second principal plane, and AL is the axial length. In short, according to the Littman formula, $D_t$ can be expressed as $D_t = p*q*D_m$, where p*q is the overall image magnification. The factor $q$ can be determined from the Bennett formula: $q = 0.01306*(AL-1.82)$. The factor $p$, can be calculated from the Bennett formula if the axial length at which $D_t = D_m$ is known (24.46 mm). When $D_t = D_m$, then $p = 1/q$ and therefore, $p = 1/[0.01306(23.82 – 1.82)] = 3.38$. Thus the adjustment in magnification factor was correted by $D_t^2/D_m^2 = 0.001949*(AL-1.82)^2$.

### Statistical Analysis

All data was analyzed with STATA 13.0 statistical package (StataCorp LP, College Station, TX, USA). Univariate linear regression was performed to investigate the correlation between OCTA quantitative metrics and the level of induced WTR astigmatism. We included fixed effects for each individual eye in order to use variation within an individual eye to estimate the effect of astigmatism on the outcome variables. By using fixed effects for our linear regressions, we accounted for variation in axial length (along with variation with any other possible confounding variable for which we are unaware) between eyes. Therefore, we used within variation versus variation across eyes allowing us to focus only on the variability within a given eye. Additionally, standard errors were clustered on the eye level to account for the correlation in errors within each eye. All continuous variables are presented as mean ± standard deviation, unless otherwise stated. P-value of less than 0.05 was considered to be statistically significant.

## Results

A total of 15 eyes from 15 patients met the inclusion criteria and were recruited for this study (Table 1). The average age was 40.9 years old, with a nearly equal distribution of right

vs left eyes (47% right eyes), and males vs females (47% males). All eyes were phakic, with an average axial length of 24.32 mm (± 1.3, range 22.72–27.10), average spherical equivalent refractive error of −2.43 D (± 2.91, range −8 to +2.25), and average SD-OCTA signal strength of 9.7 (± 0.6, range 8–10).

The effects of induced astigmatism on FAZ, VD, and PD measurements are summarized in Table 2. Induced astigmatism did not result in any significant changes to FAZ size ($p = 0.85$), perimeter ($p = 0.54$), or circularity ($p = 0.11$). Each 1 D increase in induced astigmatism was associated with a 0.46 $mm^{-1}$ decrease in central ring VD ($p = 0.002$), 0.54 $mm^{-1}$ decrease in inner ring VD ($p < 0.001$) and 0.53 $mm^{-1}$ decrease in full ring VD ($p < 0.001$); sub-region analysis within the inner ring further indicated a 0.57 $mm^{-1}$ decrease in ETDRS inner superior field VD ($p < 0.001$), 0.51 $mm^{-1}$ decrease in ETDRS inner inferior field VD ($p < 0.001$), 0.63 $mm^{-1}$ decrease in ETDRS inner nasal field VD ($p < 0.001$) and 0.45 $mm^{-1}$ decrease in ETDRS inner temporal field VD ($p = 0.003$) for each 1 D increase in induced astigmatism. Figure 1 is a representative example of the VD measurements from the lower end of the spectrum, showing minimal changes induced in a right eye with no induced WTR astigmatism (A), 0.75 D WTR astigmatism (B), 1.75 D WTR astigmatism (C), and 2.75 D WTR astigmatism (D). Figure 2 is a representative example of the upper end of the spectrum, that shows greater changes induced in a left eye with increasing levels of WTR astigmatism: 0.00 (A), 0.75 D (B), 1.75 D (C) and 2.75 D (D). Lastly, Figure 3 is a representative example of the VD measurements from the middle of the spectrum, showing mid-range changes induced in horizontal inner subfields of a right eye with increasing levels of WTR astigmatism: 0.00 (A), 0.75 D (B), 1.75 D (C) and 2.75 D (D). Each 1 D increase in induced astigmatism was associated with a 0.0080 decrease in central ring PD ($p = 0.004$), 0.0072 decrease in inner ring PD ($p < 0.001$) and 0.0073 decrease in full ring PD ($p < 0.001$); sub-region analysis within the inner ring further indicated a 0.0074 decrease in ETDRS inner superior field PD ($p = 0.002$), 0.0064 decrease in ETDRS inner inferior field PD ($p < 0.001$), 0.0089 decrease in ETDRS inner nasal field PD ($p = 0.001$) and 0.0061 decrease in ETDRS inner temporal field PD ($p = 0.022$) for each 1 D increase in induced astigmatism. The effect of induced WTR astigmatism was more symmetric for vertical quadrants and asymmetric for horizontal quadrants. For both VD and PD, vertical changes were intermediate, while nasal changes were the greatest, and temporal changes the smallest. Specifically, for vertical quadrants, the resulting decrease (in response to a 1 D increase in induced WTR astigmatism) in the superior quadrant was 12% greater in magnitude for VD and 16% greater for PD than the inferior quadrant. In contrast, for horizontal quadrants, the differences were much larger in magnitude. Specifically the resulting decrease (in response to a 1 D increase in induced WTR astigmatism) in the nasal quadrant was 40% greater in VD and 48% greater in PD than the temporal quadrant.

## Discussion

In this study, we evaluated the effect of induced WTR astigmatism on SD-OCTA quantitative metrics, in healthy eyes with no intraocular pathologies. Each 1 D increase in induced WTR astigmatism resulted in a generalized decrease in both VD and PD across all subfields within the 3×3mm scan area, while having no significant effect on FAZ metrics. In the horizontal axis, VD and PD depression were greater in the nasal than temporal

quadrants. In the vertical axis, VD and PD depression were greater in the superior than inferior quadrants. Comparing horizontal and vertical axes, VD and PD depression occurred more symmetrically within the vertical quadrants than within the horizontal quadrants.

The findings of this study suggest that the presence of optical astigmatism results in an underestimation of VD and PD values based on SD-OCTA, which are in keeping with previous reports of a generalized reduction in measured VD and PD values following spherical defocus.[29] In a study of a single patient by Tomlison and colleagues,[29] it was demonstrated that a spherical defocus of −3.0 D resulted in a 10.4% decrease in VD measured by the AngioVue OCTA (Optovue, Fremont, CA, USA), despite acceptable quality readouts for all images. The effect of incorrect focus limits the ability to visualize fine capillary vessels and causes an apparent thickening of the remaining vasculature.[29] Current OCTA software can correct for spherical refractions, but not astigmatism. The clinical implication of this effect is likely to be relevant only when considering the use of SD-OCTA for the evaluation of retinal pathologies in eyes with significant cylindrical refractive errors, as may be seen in pathologies such as keratoconus and other corneal ectasias. In this study, we induced WTR astigmatism up to 2.75 D but on average, the corneal astigmatism in keratoconus is 4.0 D.[40,41] The use of SD-OCTA in these keratoconic eyes without appropriate refractive correction for optical astigmatism may result in inaccurately depressed VD and PD values in select quadrants. In addition, even mild keratoconus can progress in 25% of cases,[41] leading to worsening cylindrical refractive errors over time, thus affecting the validity of OCTA cross-comparisons during longitudinal follow up. Although this effect may be more significant in eyes with corneal astigmatism greater than 3.0 D, there is likely less of an effect in the general population as the average corneal astigmatism is typically around 0.50 to 1.50 D;[42,43] but caution should be noted when following quantitative OCTA metrics longitudinally as the average astigmatism may increase and change with age from WTR to against-the-rule (ATR) astigmatism.[43] Additionally, patients who have undergone surgical procedures such as cataract extraction surgery, pterygium stripping and other refractive procedures may experience a sudden and significant change in their cylindrical refractive errors, which precludes an accurate comparison of OCTA scans acquired pre- versus post-procedure.

In this study, the placement of toric contact lenses of increasing powers (0.75, 1.75 and 2.75 D) induced WTR astigmatism of increasing magnitude. WTR astigmatism results in a horizontal optical defocus, which results in a greater obscuration of anatomical structures with a horizontal orientation than structures that are oriented vertically (Figure 1–3). Liu and colleagues previously evaluated the effect of WTR astigmatism on optical coherence tomography retinal nerve fiber layer (RNFL) measurements and noted that the eyes with higher levels of astigmatism had the appearance of a larger disc and rim area, thinner RNFL in the temporal quadrant, and farther temporally-positioned superotemporal and inferotemporal peak locations of RNFL thickness.[44] The effect of corneal astigmatism also resulted in an enhanced magnification effect resulting in an optic disc that appeared more vertically oval, and an inaccurate, horizontal displacement of the scanning circle from the optic disc, leading to an artificially-decreased RNFL thickness measurement.[44] Additionally, Hwang et al.[45] also induced WTR and ATR astigmatism with soft toric contact lenses and demonstrated that RNFL thicknesses of superior and inferior areas decreased after induction

of a WTR astigmatism, and RNFL thickness of nasal and temporal areas decreased after induction of an ATR astigmatism. By inducing significant degrees of astigmatism, this changed the scan distance from the optic disc and led to alterations in the RNFL thickness measurements.[45]

In the present study, we analyzed the effect of induced WTR astigmatism on quantitative measurements of the superficial retinal capillary vasculature. There may be an anatomic basis for our findings. On a general and macroscopic level, similar to retinal ganglion cells, retinal superficial capillary vasculature follows a predominantly horizontal orientation nasal to the fovea, gradually transiting to a near-vertical orientation temporal to the fovea, while following an intermediate orientation in the regions superior and inferior to the fovea.[46] On a microscopic level, however, it is apparent that horizontally-oriented vessels can be found and imaged within the SRL at all regions around the fovea, especially amongst finer vessels within the higher order branches of the capillary bed.[47] We found that induced WTR astigmatism resulted in selective obscuration of horizontally-oriented retinal capillary vasculature which was present in all ETDRS quadrants, thus leading to progressively and globally reduced quantitative metrics with increased diopters of astigmatism. The observation of a disparately larger effect of increased induced astigmatism on VD and PD reduction in the nasal quadrant can additionally be explained by the fact that the nasal quadrant naturally has, as explained above, a higher density of horizontally-oriented SRL capillaries.

Current OCTA systems use an ocular lens to bring the retina into focus for a wide range of spherical refractive errors, but do not correct for the meridional effects of astigmatism-induced magnification errors. The mathematical correction of spherical refraction-induced image magnification is based on the Littmann formula,[48] which was first described in 1982 and subsequently refined by Bennett and colleagues in 1994.[49] The Littman formula states that the true anatomical dimension of a retinal feature (t) is dependent on an interaction between the measured dimension (s), camera magnification factor (p) and ocular magnification factor (q).[44] In determining the effects of ametropia on the ocular magnification factor (q), any existing astigmatism is most commonly dealt with by collapsing the optical powers along the two principal axes into a single, spherical equivalent term while ignoring the axis direction. While this is a common practice, it nonetheless results in a masking of the actual meridional effects of astigmatism-induced magnification errors, which emerges as a key consideration especially when making comparisons of dimension sizes between orthogonally-oriented anatomical features such as SRL capillaries in different anatomical quadrants.

This study provides important information about the ability to reliably analyze quantitative metrics in eyes with induced astigmatism. Despite the presence of statistically significant effects of increasing astigmatism on OCTA metrics, the amount of reduction in VD and PD is relatively small even up to an induced astigmatism of 2.75 D. As such, uncorrected astigmatism may have a limited effect on the overall reliability and reproducibility of OCTA metrics for most patients. However, such a measurement error may increase and effectively shift location as the cornea develops more ATR astigmatism with age. In addition, this effect will be expected to be exacerbated and therefore more clinically relevant especially in

pathological corneal ectatic conditions such as keratoconus, in which the average baseline corneal astigmatism is known to be greater than 3.0 D, with a possibility of progression to a range of 10 to 15 D in extreme cases.[41,50]

We acknowledge the study's limited sample size with relatively small number of eyes and the limitations of utilizing only the AngioPlex (Carl Zeiss Meditec, Inc., Dublin, CA, USA) SD-OCTA system, and thus the results may not be reproducible across other commercial platforms. Even with a small sample size, this exploratory study achieved statistical significance across a vast majority of our regression analyses and appeared more than sufficient for analyzing the included outcome variables. Furthermore, we did include eyes with, on average, −2.43 D of myopia. However, the effect of this defocus was mitigated by adjusting the spherical focus on the SD-OCTA during image acquisition, which utilizes a telecentric lens that allows for a standard field of view for all images acquired. The effect of magnification due to variability in axial lengths may also affect the quantification of vessel density metrics, and to confirm our statistical approaches were robust, we adjusted for axial length-induced magnification based on the findings of Sampson and colleagues. In addition, the effect of axial length on the parafoveal superficial retinal vessel density is relatively small, ranging from −3% to +2% for a refractive error ranging from −8.00 D to +4.88 D and axial length from 21.27 to 28.85 mm.[30] In their study, the included eyes had a greater range in refractive error and axial length than what was noted in this present study (refractive range of −8.00 D to +2.25 D and axial length 22.72 to 27.10 mm. This minimal loss of data (or gain of data) contained within the ETDRS parafoveal inner ring due to magnification issues was also fully accommodated statistically with the fixed effects used for the linear regression analysis, which allows us to focus on the changes within the ETDRS inner subfields within a given eye across the 4 levels of induced astigmatism (0, +0.75, +1.75 and +2.75). Moreover, our sub-analysis was comparing intra-eye changes in the vertical (superior and inferior) versus horizontal (nasal and temporal) subfields, and not inter-eye changes, which are at higher risk for this confounding effect. Lastly, automated segmentation boundaries could lead to possible segmentation errors and affect the quantitative metrics analysis. We attempted to minimize the amount of artifact errors by utilizing healthy, normal eyes with high quality, correctly segmented and focused images, and strong signal strength.

In conclusion, our study is the first to demonstrate the qualitative and quantitative effects of induced astigmatism on SD-OCTA SRL metrics. Measurements within the entire macula are affected by induced WTR astigmatism, but most significantly so nasally. Astigmatic shifts are likely to confound both time-based and meridional cross-comparisons of these measurements, especially in the presence of high astigmatic errors.

## Supplementary Material

Refer to Web version on PubMed Central for supplementary material.

## Acknowledgements

a) Funding/Support: This work was supported in part by an unrestricted grant from Research to Prevent Blindness (RPB), K08 Grant (QVH, 1 K08 EY023595, National Eye Institute, NIH) and National Medical Research Council

(NMRC) Clinician Scientist Award Grant (QVH, CSA-INVMay0011, Singapore). The sponsor or funding organization had no role in the design or conduct of this research.

b) Financial Disclosures: JJJ: Consultant: Carl Zeiss Meditec, Inc., Alimera Sciences, Allergan, Google; YQS: No financial disclosures; PS, SY, MKD: Employment: Carl Zeiss Meditec; QVH: Johnson & Johnson

c) Design of the study (JJJ, PS, QVH), Conduct of the study (JJJ, PS, SY), Collection of the data (SY, PS), Management of the data (JJJ, YQS, PS, QVH), Analysis of the data (JJJ, YQS, SY, PS, MKD, QVH), Interpretation of the data (JJJ, YQS, PS, MKD, QVH), Preparation of the manuscript (JJJ, YQS, QVH), Review of the manuscript (JJJ, YQS, PS, SY, MKD, QVH), and Approval of the manuscript (JJJ, YQS, PS, SY, MKD, QVH).

d) Approval was obtained from the Salus IRB (Austin, TX, USA) for this Health Insurance Portability and Accountability Act-compliant, retrospective cohort study, and all research adhered to the tenets of the Declaration of Helsinki. IRB was completed prospectively and approved the research design.

## Biographies

Jesse Jeno Jung, M.D. is currently a Partner at East Bay Retina Consultants and a volunteer Clinical Instructor at University of California, San Francisco Dept. of Ophthalmology. He completed his Ophthalmology residency and was Chief Resident at New York University School of Medicine/Manhattan Eye, Ear, and Throat Hospital (MEETH) and vitreoretinal fellowship at the Edward S. Harkness Eye Institute, Columbia University College of Physicians and Surgeons/Vitreous Retina Macula Consultants of New York/MEETH.

Quan (Donny) V. Hoang, M.D., Ph.D. is a clinician-scientist, vitreoretinal surgeon and Asst. Professor at the Singapore Eye Research Institute, Singapore National Eye Centre, Duke-NUS Medical School, Singapore and adjunct Asst. Prof. of Ophthalmology at Columbia University, New York. His clinical and laboratory-based research focuses on elucidating the biomechanical changes underlying High and Pathologic Myopia and developing novel treatment modalities for these diseases.

## References

1. Spaide RF, Fujimoto JG, Waheed NK, Sadda SR, Staurenghi G. Optical coherence tomography angiography. Prog Retin Eye Res. 2018;64:1–55. [PubMed: 29229445]
2. Migacz JV, Gorczynska I, Azimipour M, Jonnal R, Zawadzki RJ, Werner JS. Megahertz-rate optical coherence tomography angiography improves the contrast of the choriocapillaris and choroid in human retinal imaging. Biomed Opt Express. 2019;10(1):50–65. [PubMed: 30775082]

3. Spaide RF, Klancnik JM, Cooney MJ. Retinal vascular layers imaged by fluorescein angiography and optical coherence tomography angiography. JAMA Ophthalmol. 2015;133(1):45–50. [PubMed: 25317632]
4. Yannuzzi LA, Rohrer KT, Tindel LJ, et al. Fluorescein angiography complication survey. Ophthalmology. 1986;93(5):611–617. [PubMed: 3523356]
5. Karhunen U, Raitta C, Kala R. Adverse reactions to fluorescein angiography. Acta Ophthalmol. 1986;64(3):282–286. [PubMed: 2944349]
6. Jung JJ, Chen MH, Lee SS. Branch Retinal Artery Occlusion Imaged With Spectral-Domain Optical Coherence Tomographic Angiography. JAMA Ophthalmol. 2016;134(4):e155041. [PubMed: 27078016]
7. Kogo T, Muraoka Y, Iida Y, et al. Angiographic Risk Features of Branch Retinal Vein Occlusion Onset as Determined by Optical Coherence Tomography Angiography. Invest Ophthalmol Vis Sci. 2020;61(2):8.
8. Ogasawara Y, Iwase T, Yamamoto K, Ra E, Terasaki H. Relationship Between Abnormalities Of Photoreceptor Microstructures And Microvascular Structures Determined By Optical Coherence Tomography Angiography In Eyes With Branch Retinal Vein Occlusion. Retina. 2020;40(2):350–358. [PubMed: 31972806]
9. Sakimoto S, Kawasaki R, Nishida K. Retinal Neovascularization–Simulating Retinal Capillary Reperfusion in Branch Retinal Vein Occlusion, Imaged by Wide-Field Optical Coherence Tomography Angiography. JAMA Ophthalmol. 2020;138(2):216–218. [PubMed: 31830212]
10. Nagasato D, Tabuchi H, Masumoto H, et al. Automated detection of a nonperfusion area caused by retinal vein occlusion in optical coherence tomography angiography images using deep learning. PloS One. 2019;14(11):e0223965. [PubMed: 31697697]
11. Jung JJ, Chen MH, Shi Y, et al. Correlation Of En Face Optical Coherence Tomography Angiography Averaging Versus Single-Image Quantitative Measurements With Retinal Vein Occlusion Visual Outcomes. Retina doi: 10.1097/IAE.0000000000002453. 22 1 2019.
12. Arrigo A, Romano F, Aragona E, et al. Optical Coherence Tomography Angiography Can Categorize Different Subgroups Of Choroidal Neovascularization Secondary To Age-Related Macular Degeneration. Retina doi: 10.1097/IAE.0000000000002775. 6 2 2020.
13. Hikichi T, Agarie M, Kubo N, Yamauchi M. Predictors Of Recurrent Exudation In Choroidal Neovascularization In Age-Related Macular Degeneration During A Treatment-Free Period. Retina doi: 10.1097/IAE.0000000000002745. 7 1 2020.
14. Faatz H, Farecki M-L, Rothaus K, Gutfleisch M, Pauleikhoff D, Lommatzsch A. Changes in the OCT angiographic appearance of type 1 and type 2 CNV in exudative AMD during anti-VEGF treatment. BMJ Open Ophthalmol. 2019;4(1):e000369.
15. Yeo JH, Chung H, Kim JT. Swept-Source Optical Coherence Tomography Angiography According to the Type of Choroidal Neovascularization. J Clin Med 2019;8(9): 1272.
16. de Jong JH, Braaf B, Amarakoon S, et al. Treatment Effects in Retinal Angiomatous Proliferation Imaged with OCT Angiography. Ophthalmologica 2019;241(3):143–153. [PubMed: 30227415]
17. Le Rouic J-F, Peronnet P, Barrucand A, et al. [Indications for fluorescein angiography and optical coherence tomography angiography (OCTA) in medical retina: Changes from 2015 and 2018]. J Fr Ophtalmol 2 2020.
18. Cheung CMG, Yanagi Y, Akiba M, et al. Improved Detection And Diagnosis Of Polypoidal Choroidal Vasculopathy Using A Combination Of Optical Coherence Tomography And Optical Coherence Tomography Angiography. Retina 2019;39(9):1655–1663. [PubMed: 29927796]
19. Zahid S, Chen KC, Jung JJ, et al. Optical Coherence Tomography Angiography Of Chorioretinal Lesions Due To Idiopathic Multifocal Choroiditis. Retina 2017;37(8):1451–1463. [PubMed: 27880741]
20. Dutheil C, Korobelnik J-F, Delyfer M-N, Rougier M-B. Optical coherence tomography angiography and choroidal neovascularization in multifocal choroiditis: A descriptive study. Eur J Ophthalmol. 2018;28(5):614–621. [PubMed: 29569477]
21. Sandhu HS, Elmogy M, El-Adawy N, et al. Automated diagnosis of diabetic retinopathy using clinical biomarkers, optical coherence tomography (OCT), and OCT angiography. Am J Ophthalmol. doi: 10.1016/j.ajo.2020.01.016. 23 1 2020.

22. Marques IP, Alves D, Santos T, et al. Characterization of Disease Progression in the Initial Stages of Retinopathy in Type 2 Diabetes: A 2-Year Longitudinal Study. Invest Ophthalmol Vis Sci. 2020;61(3):20.

23. Forte R, Haulani H, Jürgens I. Quantitative And Qualitative Analysis Of The Three Capillary Plexuses And Choriocapillaris In Patients With Type 1 And Type 2 Diabetes Mellitus Without Clinical Signs Of Diabetic Retinopathy: A Prospective Pilot Study. Retina. 2020;40(2):333–344. [PubMed: 31972804]

24. Choi EY, Park SE, Lee SC, et al. Association Between Clinical Biomarkers and Optical Coherence Tomography Angiography Parameters in Type 2 Diabetes Mellitus. Invest Ophthalmol Vis Sci. 2020;61(3):4.

25. Battista M, Borrelli E, Sacconi R, Bandello F, Querques G. Optical coherence tomography angiography in diabetes: A review. Eur J Ophthalmol doi: 10.1177/1120672119899901. 12 1 2020.

26. Holmen IC, Konda MS, Pak JW, et al. Prevalence and Severity of Artifacts in Optical Coherence Tomographic Angiograms. JAMA Ophthalmol. doi: 10.1001/jamaophthalmol.2019.4971. 5 12 2019.

27. Spaide RF, Fujimoto JG, Waheed NK. Image Artifacts In Optical Coherence Tomography Angiography. Retina Phila Pa 2015;35(11):2163–2180.

28. Lim HB, Kim YW, Kim JM, Jo YJ, Kim JY. The Importance of Signal Strength in Quantitative Assessment of Retinal Vessel Density Using Optical Coherence Tomography Angiography. Sci Rep 2018;8(1):1–8. [PubMed: 29311619]

29. Tomlinson A, Hasan B, Lujan BJ. Importance of Focus in OCT Angiography. Ophthalmol Retina 2018;2(7):748–749. [PubMed: 31047385]

30. Sampson DM, Gong P, An D, et al. Axial Length Variation Impacts on Superficial Retinal Vessel Density and Foveal Avascular Zone Area Measurements Using Optical Coherence Tomography Angiography. Invest Ophthalmol Vis Sci. 2017;58(7):3065–3072. [PubMed: 28622398]

31. Holló G Influence of Posterior Subcapsular Cataract on Structural OCT and OCT Angiography Vessel Density Measurements in the Peripapillary Retina. J Glaucoma. 2019;28(4):e61–e63. [PubMed: 30946711]

32. Yu S, Frueh BE, Steinmair D, et al. Cataract significantly influences quantitative measurements on swept-source optical coherence tomography angiography imaging. PloS One. 2018;13(10):e0204501. [PubMed: 30278057]

33. De Pretto LR, Moult EM, Alibhai AY, et al. Controlling for Artifacts in Widefield Optical Coherence Tomography Angiography Measurements of Non-Perfusion Area. Sci Rep 2019;9(1):1–15. [PubMed: 30626917]

34. Li Y, Miara H, Ouyang P, Jiang B. The Comparison of Regional RNFL and Fundus Vasculature by OCTA in Chinese Myopia Population. J Ophthalmol 2018;2018:3490962. [PubMed: 29651341]

35. Leng Y, Tam EK, Falavarjani KG, Tsui I. Effect of Age and Myopia on Retinal Microvasculature. Ophthalmic Surg Lasers Imaging Retina 2018;49(12):925–931. [PubMed: 30566699]

36. Gołębiewska J, Biała-Gosek K, Czeszyk A, Hautz W. Optical coherence tomography angiography of superficial retinal vessel density and foveal avascular zone in myopic children. PloS One. 2019;14(7):e0219785. [PubMed: 31318910]

37. Saw S-M, Matsumura S, Hoang QV. Prevention and Management of Myopia and Myopic Pathology. Invest Ophthalmol Vis Sci. 2019;60(2):488–499. [PubMed: 30707221]

38. Ang M, Wong CW, Hoang QV, et al. Imaging in myopia: potential biomarkers, current challenges and future developments. Br J Ophthalmol. 2019;103(6):855–862. [PubMed: 30636210]

39. Hoang QV, Chua J, Ang M, Schmetterer L. Imaging in Myopia In: Ang M, Wong TY, eds. Updates on Myopia: A Clinical Perspective. Singapore: Springer; 2020:219–239.

40. Aslani F, Khorrami-Nejad M, Aghazadeh Amiri M, Hashemian H, Askarizadeh F, Khosravi B. Characteristics of Posterior Corneal Astigmatism in Different Stages of Keratoconus. J Ophthalmic Vis Res 2018;13(1):3–9. [PubMed: 29403582]

41. Choi JA, Kim M-S. Progression of keratoconus by longitudinal assessment with corneal topography. Invest Ophthalmol Vis Sci. 2012;53(2):927–935. [PubMed: 22247476]

42. Pontikos N, Chua S, Foster PJ, Tuft SJ, Day AC, UK Biobank Eye and Vision Consortium. Frequency and distribution of corneal astigmatism and keratometry features in adult life:

Methodology and findings of the UK Biobank study. PloS One 2019;14(9):e0218144. [PubMed: 31536508]

43. Collier Wakefield O, Annoh R, Nanavaty MA. Relationship between age, corneal astigmatism, and ocular dimensions with reference to astigmatism in eyes undergoing routine cataract surgery. Eye Lond Engl. 2016;30(4):562–569.
44. Liu L, Zou J, Huang H, Yang J, Chen S. The influence of corneal astigmatism on retinal nerve fiber layer thickness and optic nerve head parameter measurements by spectral-domain optical coherence tomography. Diagn Pathol. 2012;7(1):55. [PubMed: 22621341]
45. Hwang YH, Lee SM, Kim YY, Lee JY, Yoo C. Astigmatism and optical coherence tomography measurements. Graefes Arch Clin Exp Ophthalmol. 2012;250(2):247–254. [PubMed: 21861085]
46. Scoles D, Gray DC, Hunter JJ, et al. In-vivo imaging of retinal nerve fiber layer vasculature: imaging histology comparison. BMC Ophthalmol. 2009;9:9. [PubMed: 19698151]
47. Zhu Q, Xing X, Zhu M, et al. A New Approach for the Segmentation of Three Distinct Retinal Capillary Plexuses Using Optical Coherence Tomography Angiography. Transl Vis Sci Technol 2019;8(3):57. [PubMed: 31293812]
48. Littmann H [Determining the true size of an object on the fundus of the living eye]. Klin Monatsbl Augenheilkd. 1988;192(1):66–67. [PubMed: 3352190]
49. Bennett AG, Rudnicka AR, Edgar DF. Improvements on Littmann's method of determining the size of retinal features by fundus photography. Graefes Arch Clin Exp Ophthalmol. 1994;232(6):361–367. [PubMed: 8082844]
50. Savini G, Næser K, Schiano-Lomoriello D, Mularoni A. Influence of Posterior Corneal Astigmatism on Total Corneal Astigmatism in Eyes With Keratoconus. Cornea. 2016;35(11):1427–1433. [PubMed: 27387567]

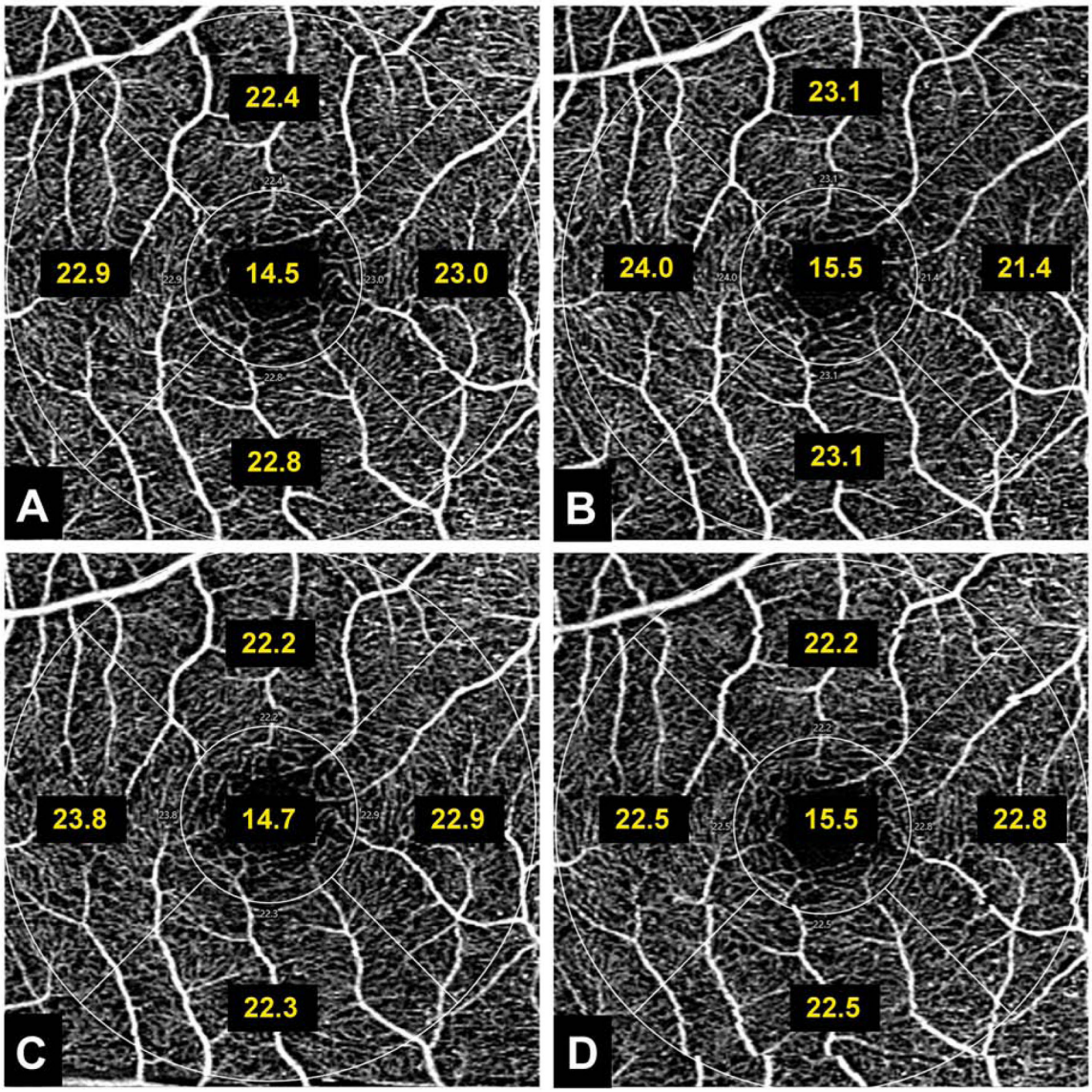


**Figure 1. Example of an OCTA scan demonstrating minimal changes in vessel density in response to induced with-the-rule astigmatism.**

A right eye representative of the lower end of the spectrum, shows minimal changes in mean values of Early Treatment of Diabetic Retinopathy Study inner subfields (yellow text) induced by increasing levels of with-the-rule astigmatism (A: 0.00, B: 0.75, C: 1.75, D: 2.75 diopters). Note the minimal difference seen between the vertical and horizontal meridian absolute values (panels A versus D). This data was among those included in the linear regression analysis to assess the magnitude and significance of association between the level of induced astigmatism and OCTA metrics, the results of which are found in Table 2.

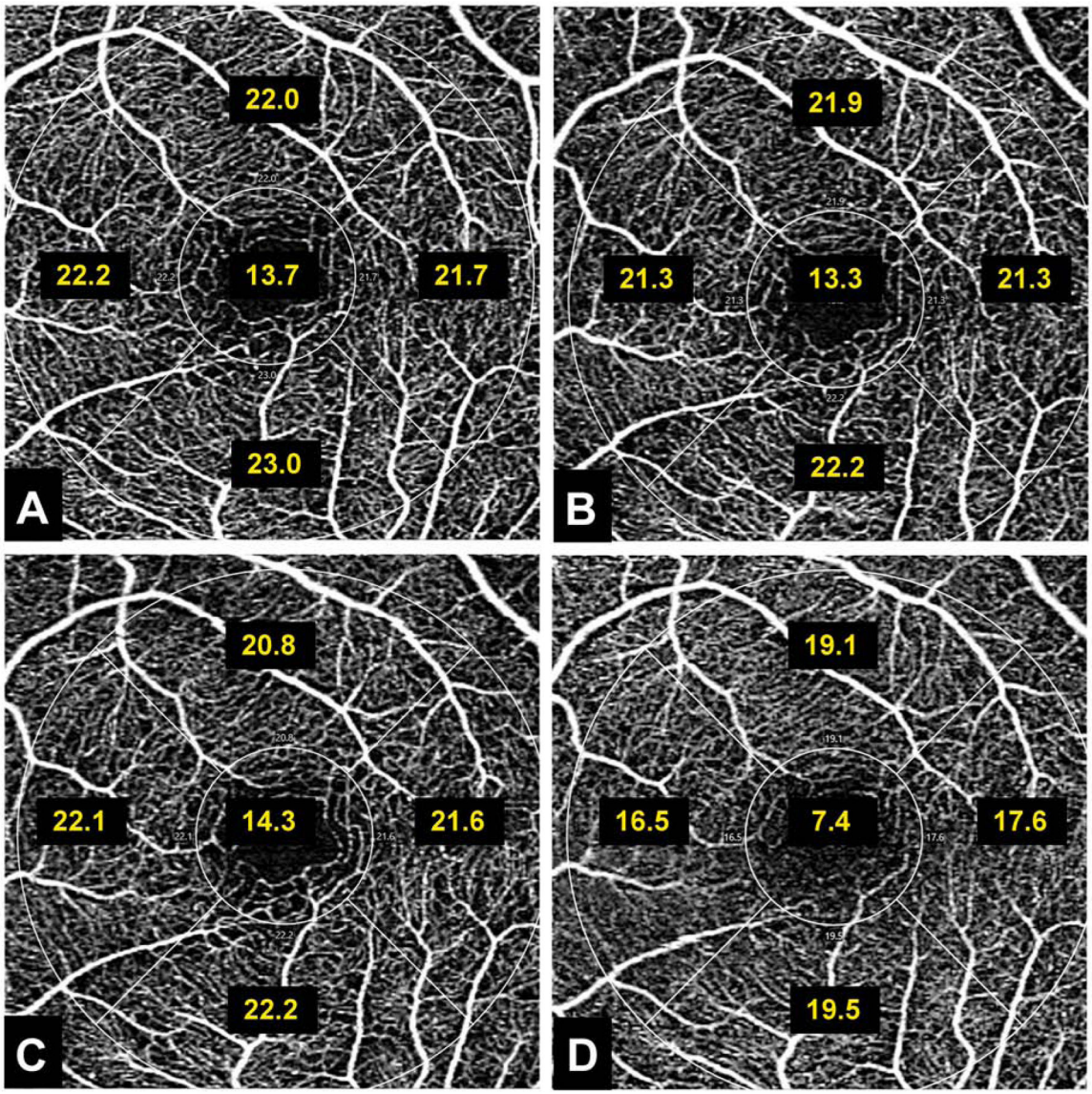


**Figure 2. Example of an OCTA scan demonstrating extreme changes in vessel density in response to induced with-the-rule astigmatism.**

A left eye representative of the upper end of the spectrum, shows maximal changes in mean values of Early Treatment of Diabetic Retinopathy Study inner subfields (yellow text), induced by increasing levels of with-the-rule (WTR) astigmatism (A: 0.00, B: 0.75, C: 1.75, D: 2.75 diopters). Vessel density values were similar when comparing vertical and horizontal meridians, under conditions of no induced astigmatism (panel A). Under the influence of 2.75D of induced astigmatism (panel D), vessel density values were more affected in the horizontal meridian than the vertical meridian. This data was among those included in the linear regression analysis to assess the magnitude and significance of association between the level of induced astigmatism and OCTA metrics, the results of which are found in Table 2.

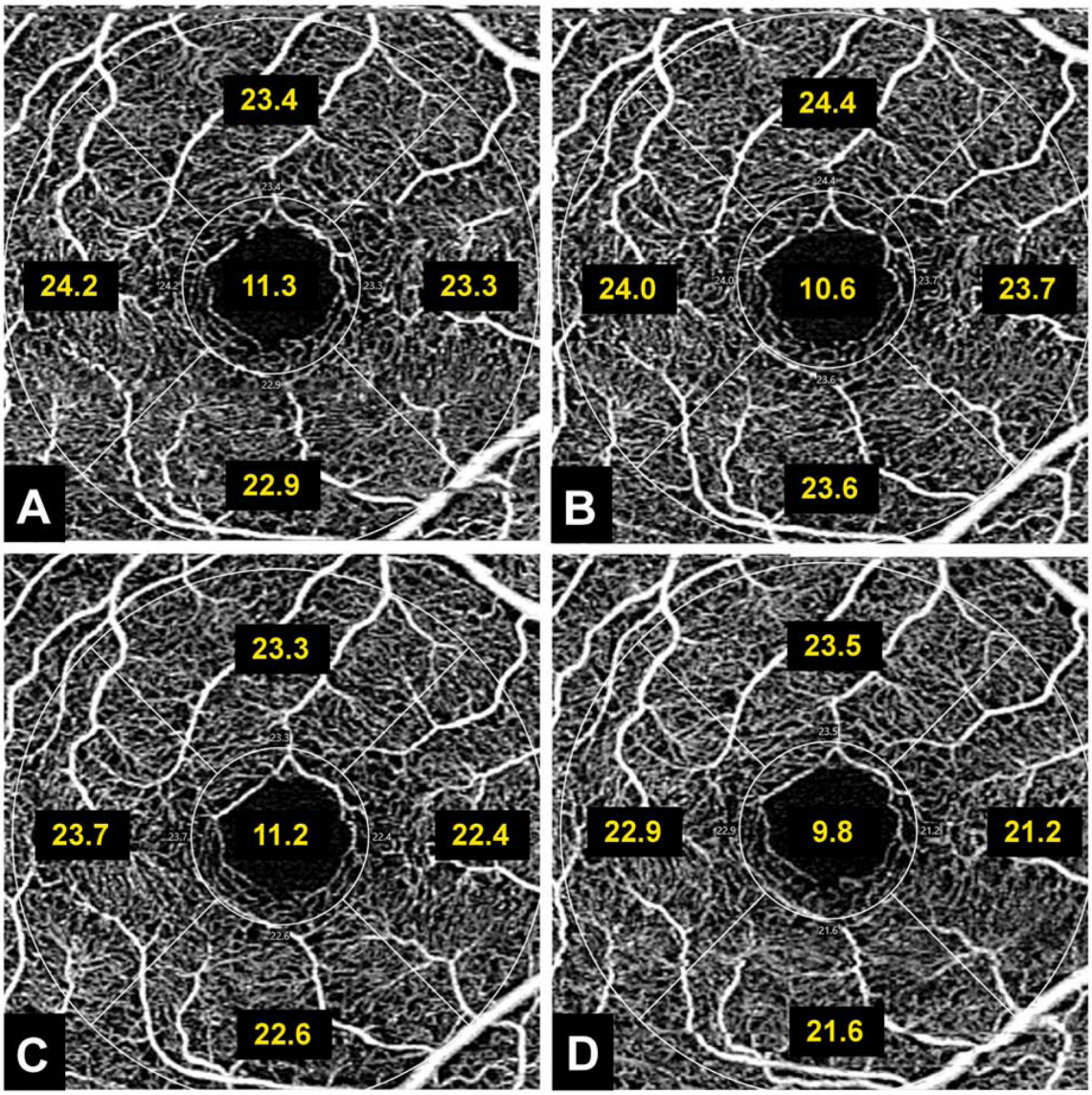


**Figure 3. Example of an OCTA scan demonstrating mid-range changes in vessel density in response to induced with-the-rule astigmatism**

A right eye representative of the middle of the spectrum, shows mid-range changes* (*mid-range values differed between horizontal and vertical meridians; for the purpose of this illustration, mid-range values refer to those observed within horizontal Early Treatment of Diabetic Retinopathy Study (ETDRS) inner subfields) in mean values of ETDRS inner subfields (yellow text), induced by increasing levels of with-the-rule astigmatism (A: 0.00, B: 0.75, C: 1.75, D: 2.75 diopters). Note the relatively larger changes (comparing panels A and D) in horizontal subfields (nasal and temporal) versus vertical subfields (superior and inferior). This data was among those included in the linear regression analysis to assess the magnitude and significance of association between the level of induced astigmatism and OCTA metrics, the results of which are found in Table 2.

**Table 1.**

Demographics

| | |
|---|---|
| Total number of eyes (n) | 15 |
| Age (years) | 40.9 (±12.8) |
| Laterality (right eye) | 7 (47%) |
| Gender (male) | 7 (47%) |
| Lens Status (phakic) | 15 (100%) |
| Axial Length (mm) | 24.32 (±1.3, Range 22.7–27.10) |
| Spherical Equivalent Refraction (diopters) | −2.43 (±2.91, Range −8 to +2.25) |
| Signal Strength | 9.7 (±0.6, Range 8 to 10) |

mm = millimeter; n = number

**Table 2.**

Univariate Analysis of Changes in Quantiative Metrics due to Induced With-the-Rule Astigmatism

| Variable | Regression Coefficient[a] | P |
|---|---|---|
| *Foveal Avascular Zone (FAZ), mean values* | | |
| Size ($mm^2$) | −0.0003 | 0.85 |
| Perimeter (mm) | 0.0062 | 0.54 |
| Circularity | −0.0065 | 0.11 |
| *Vessel Density (VD), mean values ($mm^{-1}$)* | | |
| Central Ring | −0.46 | **0.002*** |
| Inner Ring | −0.54 | < **0.001*** |
| Full Ring | −0.53 | < **0.001*** |
| ETDRS Inner Superior Field | −0.57 | < **0.001*** |
| ETDRS Inner Inferior Field | −0.51 | < **0.001*** |
| ETDRS Inner Nasal Field | −0.63 | < **0.001*** |
| ETDRS Inner Temporal Field | −0.45 | **0.003*** |
| *Perfusion Density (PD), mean values (unitless)* | | |
| Central Ring | −0.0080 | **0.004*** |
| Inner Ring | −0.0072 | < **0.001*** |
| Full Ring | −0.0073 | < **0.001*** |
| ETDRS Inner Superior Field | −0.0074 | **0.002*** |
| ETDRS Inner Inferior Field | −0.0064 | < **0.001*** |
| ETDRS Inner Nasal Field | −0.0089 | **0.001*** |
| ETDRS Inner Temporal Field | −0.0061 | **0.022*** |

[a]Linear regression coefficient for each variable, per 1 diopter increase in induced with-the-rule astigmatism. Bold face and (*) indicates statistical significance set at $p < 0.05$. ETDRS = Early Treatment Diabetic Retinopathy Study; FAZ = Foveal Avascular Zone; mm = millimeters; PD = Perfusion Density (unitless measure – total area of perfused vasculature per unit area in a region of measurement); VD = Vessel Density ($mm^{-1}$ – total length of perfused vasculature per unit area in a region of measurement)